Effect of Fretting Wear Damage in RF Connectors Subjected to Vibration: DC Contact Resistance and Phase-noise Response

R. Enquebecq[123], S. Fouvry[1], E. Rubiola[2], M. Collet[1],
1 Ecole Centrale de Lyon, LTDS
Lyon, France
2 Femto-ST, TF Dept,
Besançon, France

L. Petit[3], J. Legrand[3], L. Boillot[3]
3 Radiall
Voreppe, France
richard.enquebecq@radiall.com

***Abstract*—In many applications, RF connectors are subjected to severe environmental vibration. Vibration induces micro-displacements, leading to fretting wear damage in the contact. The purpose of this study is to investigate the effect of fretting wear on the microwave signal and more precisely on the additive phase noise [1, 2].**

A dedicated vibration test was developed, combining DC and microwave measurement. It consisted of a shaker, a vector network analyzer, a phase-noise analyzer using a cross-correlation technique, and a system for measuring electrical contact resistance. Degradation of phase noise by fretting wear was demonstrated. Two contributions were identified: relative fretting displacement amplitude, by fluctuating the total transmission distance, induced phase noise at the specific fretting frequency proportional to the fretting displacement; also, by inducing oxide debris in the interface, gross slip fretting wear damage decayed DC electrical contact resistance and microwave signal transmission. The study established quantitative correlations between the evolution of DC, transmission loss and phase-noise parameters.

I. Introduction

The effect of fretting wear damage on increased DC electrical contact resistance (ECR) was extensively investigated over the past decades [1, 2, 3, 4, 5]. Hannel demonstrated that, as long as the contact is running under a partial slip condition, the maintenance of a stick zone induces stable low DC ECR [6]. However, above a threshold displacement amplitude at which gross slip occurs (i.e., full sliding over the whole interface), fretting wear damage induces the formation of an oxide debris layer, increasing DC ECR. It was also shown in [7] that electrical constant resistance endurance strongly depends on the nature of the materials. For non-noble layers such as Sn, oxide debris is generated at the very beginning of gross slip sliding and electrical failure occurs almost instantaneously. By contrast, for noble layers such as Ag and Au, electrical failure is observed only when most of the coating has worn off. Although the effect of fretting wear damage on the evolution of DC ECR is now well established, the effect of such surface degradation on microwave transmission and phase-noise has been little investigated. The present study, combining DC, transmission loss and phase-noise measurements, seeks to clarify this aspect.

II. Presentation of the Microwave Connector

The connector used for the experiments was a plug-in technology. It consisted of a set of parts soldered together or force-fitted, while some other parts were "looser": e.g., socket/pin systems for compression and expansion of the mating connector. This ensured a blind guide and permanent electrical contact. But, as shown in Fig. 1, this socket/pin system led to damage in the connector. Under vibration, these moving parts were in constant friction and generated wear interfaces.

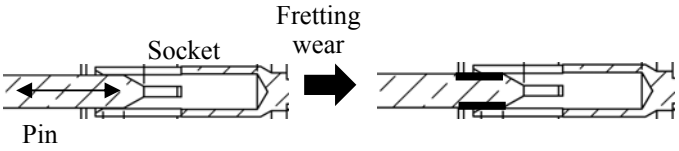

Fig. 1. Diagram of the socket/pin assembly of the connector.

III. Experiments

A. Fretting vibration test system

Fig. 2 illustrates the principle of the experiment developed at the LTDS Tribology and Systems Dynamics laboratory (Ecully, France). The pin part of the assembly was screwed on to the arm of the shaker and the socket part was glued to the frame after the pin/socket commutation. The instrumentation used to perform all the tests was composed of several elements, presented below:

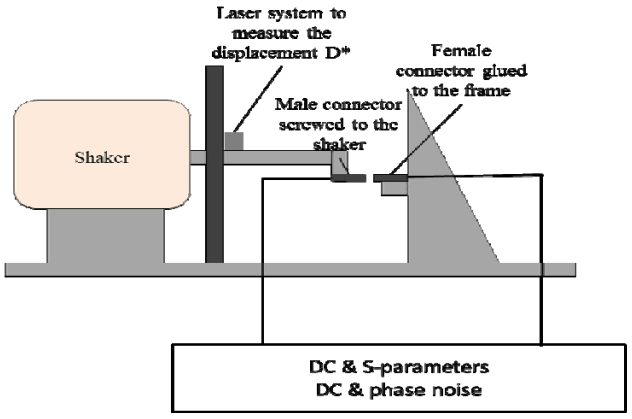

Fig. 2. Experimental measuring device

This combined screw and glue assembly method reduced the hyperstatic misalignment which could be generated if both parts were screwed. An electromagnetic shaker applied the vibration (i.e., displacement amplitude δ*) to the pin part. Frequency was set at 100 Hz and the relative displacement of the pin part was controlled using a laser sensor. A dedicated feedback system was implemented to monitor the shaker so as to impose a given displacement amplitude. Various cables were connected to the pin/socket assembly to measure the evolution of DC ECR, S_{12} transmission parameters using a VNA analyzer, and phase-noise response using a cross-correlation system, respectively. Each method is described in detail in the following:

B. Vibration analysis

To check the good mechanical design of the test bench, modal and vibration analysis was performed. Mechanical resonance can amplify phase noise, so that the noise spectrum is no longer representative of the dynamic behavior of a single connector but rather of the connector bench as a whole, with the associated mechanical supports. The device used to perform vibration analysis comprised a laser and an accelerometer, connected to a signal processing computer.

Measurement was performed with two components:

- Time domain: measurement with a sinusoidal signal to check system linearity;
- Frequency domain: to characterize the frequency response of the complete system, including the connector.

C. DC electrical contact resistance system

To characterize the evolution of DC ECR and interface damage, a common 4-wire method was adapted. (Fig. 3). Since the contact was metal-on-metal, the evolution of resistance was indicative of a change in conductivity that may be associated with surface wear and oxide debris. The 4-wire resistance measuring device included the following elements: stabilized current supply, voltmeter and amplifier.

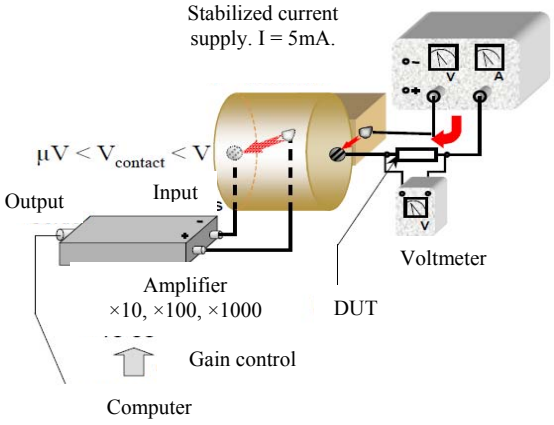

Fig. 3. Principle of 4-wire electrical contact resistance measurement [2]

The stabilized current supply generated a steady current of 5 mA. The ECR induced a voltage variation which was measured using a combined amplifier-voltmeter system. Imposing I, and measuring V, ECR variation (ΔR_{DC}) was deduced applying the Ohm law.

D. S21 loss measurement

Correlation between the evolution of the DC resistance and microwave signal properties was tested using the following elements (Fig. 4):

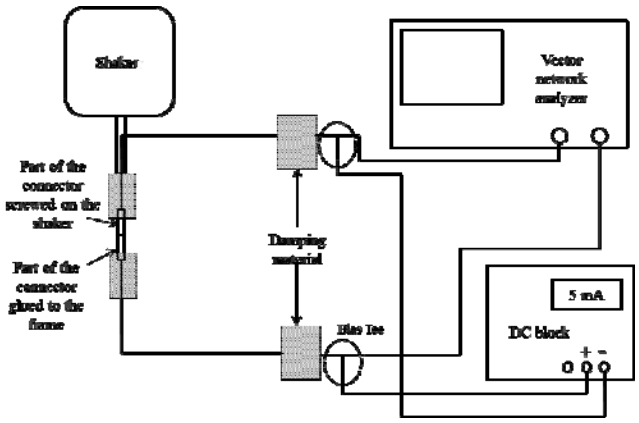

Fig. 4. Microwave and DC measurement

Vector network analyzer:

The vector network analyzer identified the microwave behavior of the connector. We will focus on the evolution of the Smith "S" parameters S_{11}, S_{22} which describe mismatch at both ports, and S_{21}, S_{12} which describe insertion loss behavior during connector wear. The real and imaginary parts enable identification of some type of parasite interactions suspected to occur at the interfaces and which can be either resistive, reactive capacitive, or inductive.

Bias tee:

The bias tee enables a DC signal to be superimposed on an HF signal. It is possible to study simultaneously the correlation between ECR, S parameters and phase noise.

E. Phase noise and measurement technique

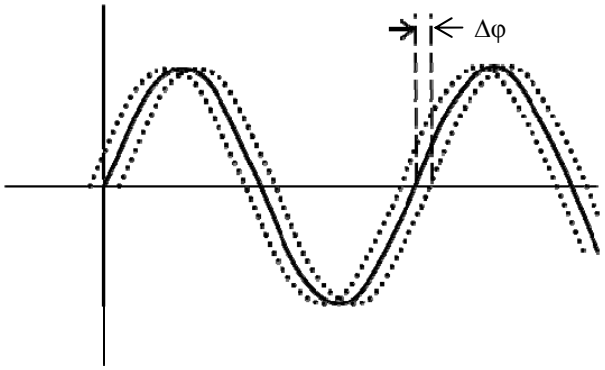

Fig. 5. Illustration of phase-noise shift

Subjected to various stresses, material damage and contact wear, a connector can induce phase-noise disturbance of the transmitted signal (Fig.5), to quantify which the following

variables are considered [8,9,10]. The temporal signal is expressed by:

$$v(t) = V_0 (1 + \alpha(t)) \cdot \cos(\omega_0 t + \varphi(t)) \qquad (1)$$

with φ(t) the fluctuation of the phase. Considering a Fourier transform, this leads to:

$$\Phi(f) = \int_{-\infty}^{\infty} \varphi(t) * e^{-i\omega t} dt \qquad (2)$$

The determination of the power spectral density in rad²/Hz is given by:

$$S\varphi(f) = (1/T)\langle \Phi(f) \cdot \Phi^*(f) \rangle_m \qquad (3)$$

Finally the phase-noise parameters used for the analysis, expressed in dBc/Hz, is provided by:

$$L(f) = \frac{1}{2} S\varphi(f) \qquad (4)$$

The phase-noise analyzer performed additive noise measurements with cross-correlation. The principle of the system is the following:

The method uses an external phase-locked loop comprising two mixers. The purpose of the technique is to overcome the noise contributions of the various electronic components of the assembly so that only the phase noise associated to the equipment under test, or DUT (Device Under Test), remains (Fig. 6).

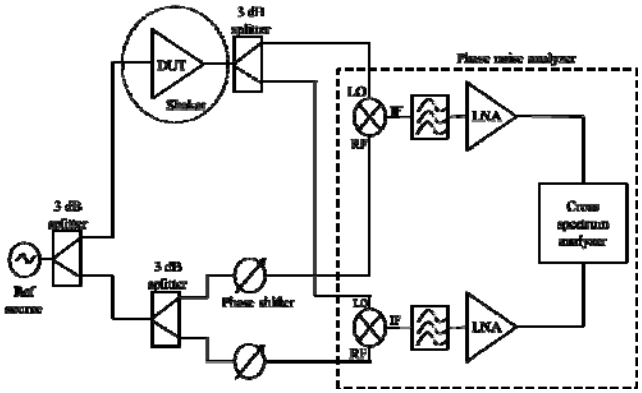

Fig. 6. Diagram of the measurement technique by cross-correlation.

The correlation technique uses two identical instruments simultaneously measuring the same DUT. The two instruments are assumed to be independent, with only the DUT in common. The DUT phase noise is correlated, while the noise of the mixers, phase shifters and LNAs is uncorrelated and averaged to a value that tends toward zero. The operation can be expressed by the following mathematical relations:

$$x(t) = c(t) + a(t) \quad y(t) = c(t) + b(t) \qquad (5)$$

where "c" represents the correlated noise corresponding to the DUT while "a" and "b" are uncorrelated noise for each channel. [9,11].

$$\langle S_{xy}(f) \rangle_m = (1/T) \langle Y X^* \rangle_m \qquad (6)$$

$$= (1/T) \langle [C + A] [C + B]^* \rangle_m$$

$$= (1/T) [\langle CC^* \rangle_m + \langle CB^* \rangle_m + \langle AC^* \rangle_m + \langle AB^* \rangle_m]$$

where A, B and C are the Fourier transforms of time domain random function a, b and c, and m is the number of spectra averaged, and T is the acquisition time.

Increasing the number of averaged spectra, the cross terms CB, AC and AB are averaged out. The noise of the mixers is rejected because they are independent and uncorrelated. Only correlated contributions to the two channels of the system are then retained. Experimentally, the two channels of the system must be properly insulated and as "identical" as possible.

The improved phase-noise floor, depending on the number m of averaged spectra, follows $1/m^{0.5}$ [13]

$$N_{meas} = N_{dut} + (N1 + N2) / (m)^{1/2} \qquad (7)$$

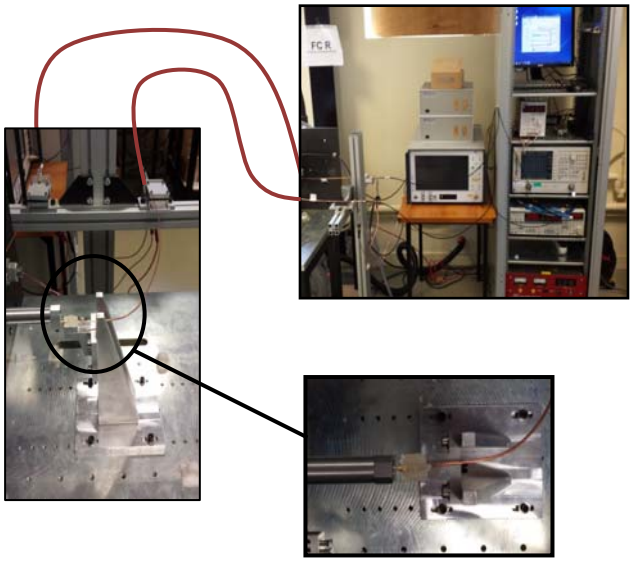

Fig. 7. Picture of the global system

Fig. 7 gives an overview of the system, including the vibration test and all the electronic devices used to measure the DC ECR, the RF signal transmission and the phase noise. DC resistance, S_{12} and phase noise could be measured independently. However, DC resistance could also be measured simultaneously with S_{21} or with the phase noise, leading respectively to DC and S_{21} or DC and phase noise configurations. Obviously, S_{12} and phase-noise analysis can be done simultaneously in a single test.

IV. Results

A. Vibration analysis

- Temporal study

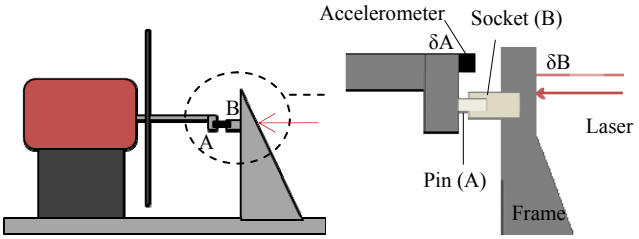

Fig. 8. Configurations studied for modal and vibration analysis

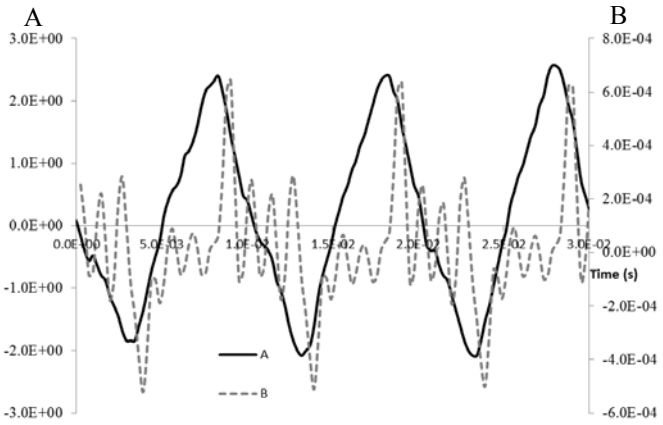

Fig. 9. Temporal response of points A and B.

The connector was coupled to the frame using the screw and glue procedure (Fig. 8). Measurement used two sensors: a laser vibrometer and an accelerometer. The accelerometer, located at the end of the shaker arm, served as reference measurement. Displacement on the pin (A) and socket (B) were measured using respectively the accelerometer and the laser vibrometer, and compared to express the relative displacement of the connector δ:

$$\delta = \delta_A - \delta_B$$

Fig. 9 shows that amplitude δ was significantly smaller than the imposed amplitude (D* = δ) due to the compliance of the frame. The signal was also more distorted than the reference displacement δ_{REF}. However, a stable sine evolution of wear was observed, confirming test procedure stability.

- Frequency response

The study focused on the connector to characterize the dynamic response generated by the connection. The frequency band excited by a random signal was between 1 and 1,600 Hz. The transfer function was measured between the laser vibrometer and the accelerometer. The laser was also pointed just behind the connector (point B).

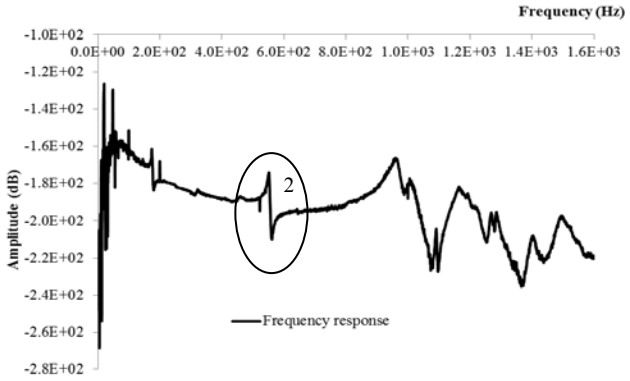

Fig. 10. Frequency response of the test bench connector plug.

The spectrum shows several modes (Fig. 10). Modes above 800 Hz were considered too complex to be easily characterized, and only mode 2 was considered (Fig. 10) and described. First, the behavior of the shaker arm was studied with the connector plugged in.

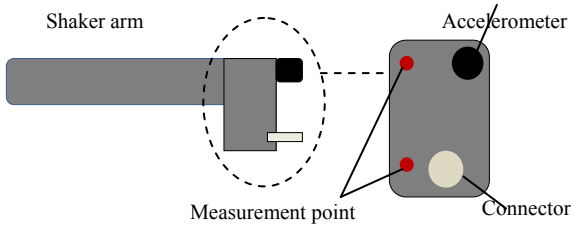

Fig. 11. Measurement points on the shaker arm.

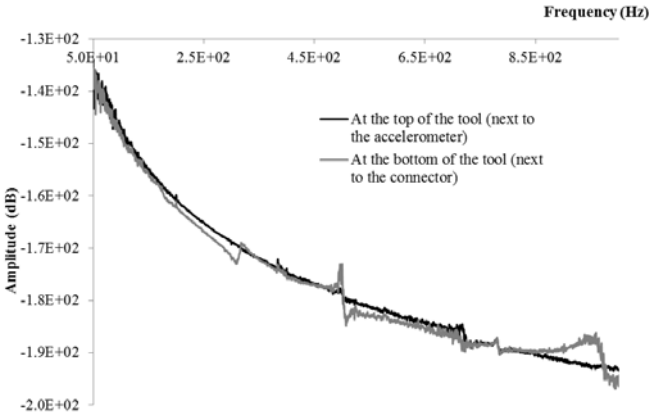

Fig. 12. Characterization of vibration modes

Two measurements were performed on the end of the arm (Fig. 11):

- one collocated next to the accelerometer;
- one on the bottom of the tool.

The collocated measurement (top of the tool) showed no resonance near the mode frequency (Fig. 12). In contrast, when the measurement was made at the bottom of the tool, certain modes were observed that were similar to those in the first spectrum (Fig. 10). It can be concluded that the corresponding mode shape corresponds to the torsion of the shaker arm induced by the connection.

B. *Identification of DC resistance evolution related to the partial/gross slip transition*

Previous investigations demonstrated that, as long as the contact was running under a partial slip condition (i.e., $\delta^* < \delta_t$), the maintenance of an unworn stick zone guaranteed stable low ECR. However, above the gross slip transition (i.e., $\delta^* > \delta_t$), the full sliding generated in the interface favored activation of an insulating oxide debris layer, decaying the ECR [2]. The transition from stable low ECR to unstable high ECR is related to the δ_t displacement amplitude transition from partial to gross slip regime. Jedrzejczyk et al. [12] showed that, for simple cross-cylinder interfaces, δt could be determined by applying a variable displacement amplitude (Fig. 8). For a given contact, displacement amplitude was increased step by step [13]. The duration of each increment was sufficient to increase ECR if the interface reached the gross slip condition. A very small initial amplitude was chosen to guarantee an initial partal slip condition. The chosen 5µm amplitude increment was sufficiently small to provide a precise estimation of δt.

The application of this approach to connectors is more complex, since the real displacement inside the pin/socket cannot be measured. However, it was shown in [14] that the contact displacement δ* is proportional to the vibration displacement on the pin D*. Therefore a similar analysis can be applied, varying D* connector displacement amplitude to determine the Dt transition from stable to unstable ECR evolution. This strategy was implemented for the studied connector, with $D_0 = \pm 15$ µm being the initial displacement, $N = 5*10^5$ cycles the duration of each plateau of the incremental evolution of D* and ΔD* = 5µm the increment of D* displacement amplitude. This fast methodology showed that the D^*_t transition of the studied connector was about ±35 µm. Above this vibration displacement amplitude, a significant increase in ECR was observed. Note that this value is significantly larger than the corresponding δ^*_t value operating in the contact: most of the displacement was accommodated by the elastic accommodation of the test system and sensor assembly.

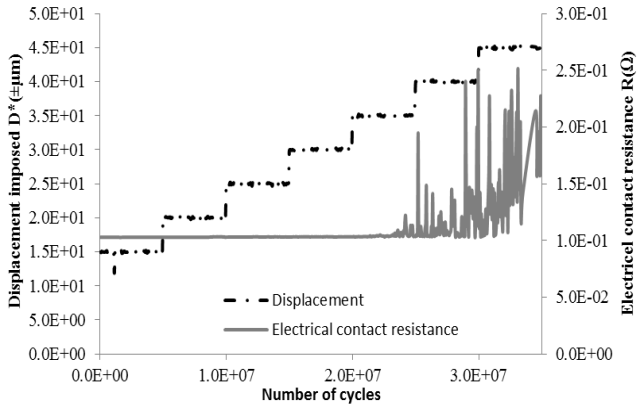

Fig. 13. Partial to gross slip transition correlated to a significant change in contact resistance

According to tests carried out on this connector, gross slip started at 35 µm amplitude (Fig. 13). The subsequent tests set the mechanical extension beyond this threshold in order to guarantee full slip displacement.

C. *Microwave loss and fretting damage evolution*

The above analysis confirmed that sliding transition from partial to gross slip promotes ECR decay by inducing surface wear and oxide debris formation. A critical question is whether this interface degradation also decays the microwave transmission. To investigate this, three connectors were tested at respectively D* = ± 15 µm, D* = ± 30 µm and D* = ± 45 µm during 15×10^6 cycles. The first condition is clearly in the partial slip regime, the second is around the transition, and the third is clearly under gross slip condition. Loss at 10 GHz and ECR were measured every 10,000 cycles. For the interpretation, test results were averaged for the first three million cycles and compared to the last three million cycles of the test. Fig. 11 plots the variation in DC ECR and S21 parameters from the beginning to the end of test 3: $\Delta R = R_f - R_i$, $\Delta S_{21} = S_{21i} - S_{21f}$. At the end of the test, the pin and clip of the sensor were optically observed. No damage was seen for D* = ±15 µm and D* = ±30 µm, whereas significant dark oxide fretting scars were observed on the specimen tested at D* = ±45 µm (Fig.14).

Fig. 14. Optical observation of the fretting scars on the connector tested at D* = ± 45 µm, $N = 15\times10^6$ cycles, f = 100 Hz.

This analysis confirmed that, under the partial slip condition, S_{21} microwave loss, like ECR, is very low. The fretting interface remained undamaged, and the maintenance of metal-metal junctions in the stick domain allowed ECR conduction and microwave transmission.

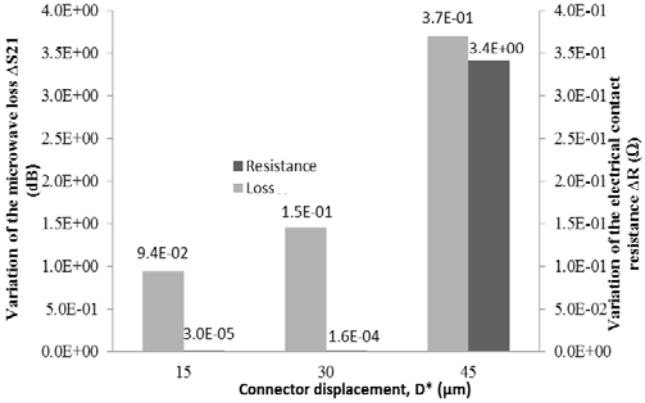

Fig. 15. Comparison between microwave loss variation and electrical contact resistance variation.

As shown in Fig. 15, both round S_{21} parameters displayed smooth increase. However, the given D value was just below the gross slip response and undamaged metal/metal stick was

still operating, inducing rather low ECR and good S_{21} microwave transmission. By contrast, for D* = ±45 µm, the gross slip within the interface, conditionally promoting an oxide debris layer, increased DC ECR but also decayed S_{21} microwave transmission. Hence, whereas at the sliding transition Δ* = ±30 µm the ECR variation ΔR was less than 1.6×10^{-4} Ω and the ΔS_{21} loss parameter variation was around 0.15 dB, they rose to respectively 3.4 Ω and 0.37 dB at Δ* = 45 µm. This result suggests that gross slip fretting wear damage, by forming a homogeneous insulating oxide debris layer trapped in the interface, not only decayed ECR but also limited microwave transmission, increasing S_{21} variation.

D. Effect of fretting wear damage on phase noise

The above analysis demonstrated that gross slip fretting wear decays S_{21} microwave transmission. A final aspect now needs to be evaluated: whether fretting wear damage can also increase phase noise. Phase noise was measured for a displacement amplitude of D* = ±45µm in two configurations (Fig. 15):

- on a new connector: after 10,000 cycles, the surfaces were undamaged and the connector was in good condition;
- on a worn connector, having undergone several million cycles: the surfaces were damaged and oxides could be seen.

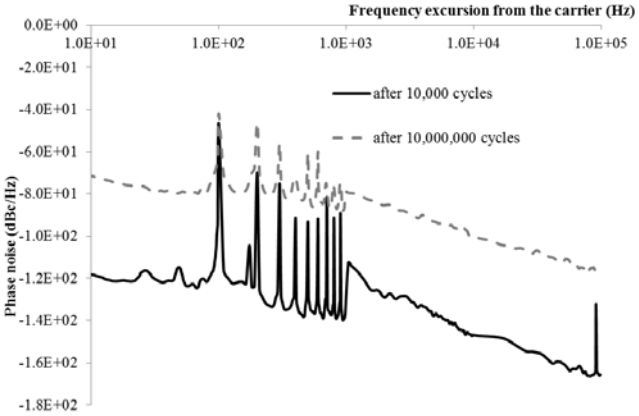

Fig. 16. Comparison of phase noise spectrum between the beginning and the end of the test for a displacement of 45 µm.

Comparison of connector noise levels between the end and the beginning of the test at a constant displacement of 45 µm (Fig. 16) clearly showed the impact of connector wear on phase noise: white noise, that gradually rising during the test while remaining below the peak amplitudes observed in the spectrum for this test. At the end of the test after 15 million cycles, the white noise due to wear had increased by approximately 40 dB. The amplitude of the fundamental peak (100 Hz) remained constant throughout during the test.

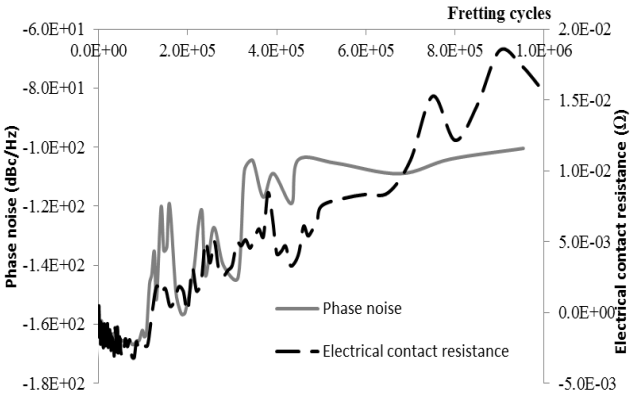

Fig 17. Evolution of phase noise and electrical contact resistance during a D* = ± 45 µm gross slip fretting vibration test (f=100 Hz).

To confirm these results, correlations between ECR and phase noise were investigated

Fig. 17 shows phase noise at 50 kHz offset from a 10 GHz carrier. The vibration on the connector was still a sinus with D*= ± 45 µm amplitude at 100 Hz. Both phase noise and DC ECR displayed similar evolution. At the beginning, phase noise and DC ECR were rather low, at respectively -1.6×10^{2} and 1.10^{-3} Ω. However, beyond 10^{5} fretting cycles, fretting wear damage, by forming an oxide debris layer, increased ECR and phase noise. After 6×10^{5} cycles, they reached respectively -1×10^{2} dB and 10^{-2} Ω. The correlation between ECR and phase noise also confirmed that, in addition to decaying ECR, the formation of on oxide debris layer trapped between the contact interfaces significantly degraded the microwave signal, by decreasing signal transmission but also by increasing phase noise disturbance.

E. Effect of electrical length variation on phase noise

We now focus on the discontineous phase noise observed at 100 Hz and succesive multiples. It is interesting to note that this phase noise discontinuity is observed at the frequency equivalent to the fretting loading frequency. Different fretting frequencies were imposed, from 25 Hz to 150 Hz, and confirmed this. To confirm the correlation between the discontineous phase noise peak and fretting displacement amplitude, two phase noise measurements were made on a new connector at a similar fretting frequency f = 100 Hz but with different displacement amplitudes. Analysis was performed after less than 10^{4} cycles, before any fretting wear damage. Fig. 18 confirms that an increase in vibration D* and related contact fretting displacement δ* induced an increase in phase-noise amplitude. Hence, of occurrence, fretting displacement controls not only the frequency of occurreence but also the amplitude of the real phase noise. This suggests that the peak phase noise observed on the phase noise spectrum (Fig. 16) was related to the variation in the distance induced by the D* fretting vibration displacement that the HF signal had to run.

In conclusion, this analysis suggests that, when subject to fretting vibration, two phase-noise contributions are activated. The first is related to fretting displacement which, by varying the total distance that the HF signal must “travel”, induces a discontineous peak in the frequency sprectrum (Fig. 16); the intensity of this peak phase noise is proportionnal to the

fretting displacement amplitude D* and related to the fretting frequency. Secondly, there is white phase noise, related to the degradation of the fretting contact where insulating oxide debris increases ECR and overall phase noise; this phase noise is independent of HF frequency. The fretting displacement phase noise depends on D* and was significantly larger than the white phase noise for the studied conditions. Further research needs to be undertaken to formalize each phase noise degradation, taking account of displacement amplitude and frequency, etc.

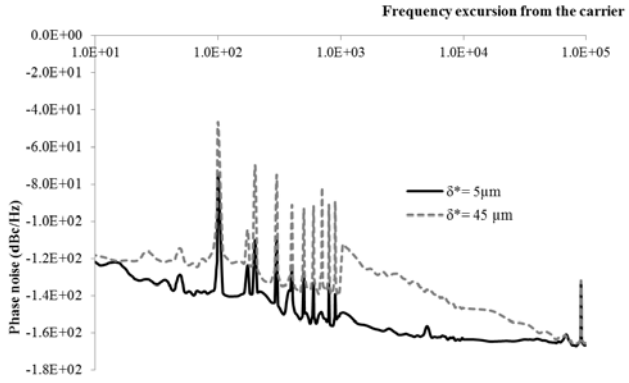

Fig. 18. Impact of change in electrical length on phase noise.

V. CONCLUSION

An original experiment was developed to investigate the effect of vibrations applied to a microwave connector in terms of the evolution of DC electrical contact resistance, transmission loss and phase noise. The following points emerged:

- The variable displacement amplitude method was able to estimate the vibration displacement threshold D_t above which gross slip wear phenomena were activated and induced an increase in DC ECR.
- Combining DC and transmission loss analysis confirmed that the gross slip fretting wear damage occurring when $D^* > D^*_t$ also decayed the microwave signal transmission loss.
- Combining DC and phase noise analysis under the gross slip condition revealed a direct correlation between increase in DC ECR and degradation of phase noise.
- Fretting displacement, by fluctuating the distance that the HF signal had to travel, induced fretting displacement phase noise, which was independent of contact degradation but directly depended on displacement amplitude and frequency. Hence two phase noise contributions were identified.

Future developments will focus on quantitative correlations between the evolution of DC, transmission loss and phase noise parameters. Other aspects (materials and surface roughness) will be also investigated.

References

[1] R. S. TIMSIT, "High Speed Electronic Connectors: A Review of Electrical Contact Propertie," IEICE Transact. Electronics, vol. E88C no. 8, August 2005.

[2] A. Kassman-Rudolphi, S. Jacobson, Tribol. Int. 30(3), 1997, pp. 165-175.

[3] A. Kassman-Rudolphi, S. Jacobson, Wear 201(1-2), 1996, pp. 244-254.

[4] N. Ben Jemaa, J. Swingler, "Correlation between wear and electrical behaviour of contact interfaces during fretting vibration," Proceedings of the 23rd ICEC conference, 2006, pp. 215-219.

[5] M. Sun, M. Rong, O. Wang, D. Chen, Proc. of the 42nd IEEE Holm Conference on EC, 1996, pp. 467-471.

[6] S. Hannel, S. Fouvry, Ph. Kapsa, L. Vincent, "The fretting sliding transition as a criterion for electrical contact performance," Wear, Volume 249, Issue 9, September 2001, Pages 761–770.

[7] S. Fouvry, P. Jedrzejczyk, P. Chalandon, "Introduction of an exponential formulation to quantify the electrical endurance of micro-contacts enduring fretting wear: Application to Sn, Ag and Au coatings," Wear, Volume 271, Issue 9-10, 2011, pp. 1524-1534.

[8] E. Rubiola, "The cross-spectrum experimental method," 27 february 2010.

[9] Simon J. Bale, David Adamson, Brett Wakley, Jeremy Everard, "Cross Correlation Residual Phase Noise Measurements using Two HP3048A Systems and a PC Based Dual Channel FFT Spectrum Analyser," 24th European Frequency and Time Forum 13-16 April 2010.

[10] E.Rubiola "Phase noise and frequency stability in oscillators," Cambridge University 2008,2010,2012.

[11] K. Gheen, "Phase Noise Measurement Methods and Techniques," Aerospace & Defense Symposium, Agilent Technologies 2012.

[12] P.Jedrzejczyk, S. Fouvry, P. Chalandon, "A fast methodology to quantify electrical-contact behavior under fretting loading conditions," Wear, volume 267, issue 9-10, September 2009, pp.1731-1740.

[13] J.M. Voisin, A.B. Vannes, L. Vincent, J. Daviot, B. Giraud, Wear 181-183, 1995, pp. 826-832.

[14] S. Fouvry, P. Jedrzejczyk, P. Chalandon, O. Alquier, "From fretting to connector vibration tests: a "transfer function" approach to predict electrical contact resistance endurance," 27th International Conference on Electrical Contacts (ICEC 2014), June 22-26, 2014, Dresden, Germany, ISBN 978-3-8007-3624-9,p. 255-260.